Structure of SDS Micelles with Propylene Carbonate as Cosolvent: a PGSE−NMR and SAXS Study

Giuseppe Colafemmina,[†,‡] Daniela Fiorentino,[†,⊥] Andrea Ceglie,[†,§] Emiliano Carretti,[†,#] Emiliano Fratini,[†,#] Luigi Dei,[†,#] Piero Baglioni,[†,#] and Gerardo Palazzo*[,†,‡]

Consorzio Interuniversitario per lo sviluppo dei Sistemi a Grande Interfase (CSGI), Firenze, Italy, Dipartimento di Chimica and Laboratorio di Ricerca per la Diagnostica dei Beni Culturali, Università di Bari, via Orabona 4, I-70126, Bari, Italy, Dipartimento STAAM, Università del Molise, v. De Sanctis, I-86100 Campobasso, Italy, Dipartimento di Chimica, Università di Firenze, via della Lastruccia 3, I-50019 - Sesto Fiorentino (FI), Italy, and Dipartimento di Scienze Biomediche, Università di Foggia, Viale Pinto, Foggia, I-71100 Italy

Received: December 22, 2006; In Final Form: March 16, 2007

The effect of propylene carbonate on SDS micelles was investigated by means of pulsed gradient spin−echo (PGSE) NMR, small-angle X-ray scattering (SAXS), conductivity and ion-selective electrode (ISE) measurements. The knowledge of the cosolvent partition between continuous phase and micelles (obtained by means of PGSE−NMR) allowed the identification of relevant dilution paths. Along these paths the system is composed of identical micelles that become more and more diluted. The extrapolation of measured self-diffusion coefficient to infinite dilution (where direct and hydrodynamic interactions are negligible) permits the determination of hydrodynamic size of the micelles. Moreover, the micelle ionization degree (measured by means of ISE) combined with PGSE−NMR and conductivity data furnishes an estimate of the aggregation number without any assumptions on micellar shape. On the other hand, troublesome hydrodynamic interactions are irrelevant to SAXS, and scattering data collected at fixed composition can be analyzed according to a reasonable model by exploiting the insight on the propylene carbonate partition gained through PGSE−NMR. By means of these approaches, we have found that propylene carbonate acts mainly as cosurfactant for the SDS micelles, decreasing their size and aggregation number by increasing the mean headgroup area of SDS.

1. Introduction

Surfactants in water spontaneously self-assemble to form micelles. The thermodynamics of micelle formation and the factors influencing the micelle size and shape were the subject of a plethora of studies in the last decades, and nowadays both topics are reasonably well understood.[1,2] However, most applications require not only surfactant and water but also some additives. In this case, the affair becomes much more complicated on a physical and semantic ground. If the added chemicals are water-insoluble (oils) we are dealing with microemulsions and the added oil forms apolar domains stabilized by the surfactant layer. Often additives are required to tune the spontaneous curvature of the surfactant layer and are termed cosurfactants; in this case, they are added only in minute amounts and partition themselves mainly at the interface (medium chain alcohols are typical examples). When the additive is miscible with water and is added in significant amounts, it is broadly termed cosolvent. The presence of a cosolvent poses some challenges to the comprehension of system microstructure. It affects the properties of the continuous aqueous phase and could be adsorbed by the surfactant layer, thus directly influencing the micelle's characteristic as well. It is worthwhile to remember that the micelle's features depends on a delicate balance of lyophobic/lyophilic interactions of the surfactant molecules with the solvent(s). Without a quantitative description of cosolvent partition between the continuous phase and micelles, ambiguity concerning its role is unavoidable. A typical example is the debate on the action mechanism of urea on micelles (chaotropic restructuring of the solvent versus direct absorption).[3,4]

In the present work we have studied the effect of propylene carbonate (PC) on SDS micelles. The motivation of the study can be traced out on the remarkable performances of mixtures made of SDS, pentanol, propilene carbonate, and water in removing vinyl polymer coating from frescoes.[5] In a previous investigation we have gained some hints on the effect of PC on the micelles structure, but a full quantitative comprehension was precluded by the presence of pentanol in the formulation.[6] Actually, micelles of SDS and pentanol in water are cylindrical and were found to evolve toward a spherical shape upon PC loading; this change of shape complicates the analysis of the results. For this reason we have turned our attention to the simplest SDS/PC/water system where micelles remain roughly spheroidal at all compositions. As stated above, the detailed description at molecular level of micelles in presence of a cosolvent is a complicated task to afford, and we were forced to develop two independent experimental approaches. The first, is based on the combination of results coming from pulsed gradient spin echo (PGSE) NMR and from two inexpensive

* Corresponding author phone: 39-080-544-2028; fax: 39-080-544-2129; e-mail: palazzo@chimica.uniba.it.
† Consorzio Interuniversitario per lo sviluppo dei Sistemi a Grande Interfase (CSGI).
‡ Università di Bari.
§ Università del Molise, v. De Sanctis.
# Università di Firenze.
⊥ Università di Foggia.

10.1021/jp0688761 CCC: $37.00
Published on Web 05/27/2007

techniques (viz. conductivity and ion-selective electrode ISE), collected along suitable dilution paths. However, at a very high PC/SDS ratio, PGSE−NMR fails to determine the diffusion coefficient of SDS and the dilution approach cannot be used. For this reason, to study the system at high PC loading we have developed a completely different approach based on the coupling of PGSE−NMR and small-angle X-ray scattering (SAXS) data.

2. Experimental Section

Sodium dodecyl sulfate (SDS) and propylene carbonate were purchased from Sigma. SDS was purified from ethanol,[4] dried under reduced pressure, and stored over dry silica gel; PC was used as received. Unless otherwise stated, all the samples where prepared by weighing.

2.1. Conductometric and ISE Measurements. Conductivity measurements were performed with a CDM230 conductivity meter (Radiometer Analytical) equipped with a 4-pole conductivity cell CDC866T (cell constant = 1.048 cm^{-1}). The free sodium ion concentration (strictly activity) was determined by potentiometric method using ion-selective electrode (ISE). The cell includes a working sodium-selective glass electrode (9650 CRISON), a reference electrode (Ag/AgCl 5241 CRISON), and was connected to a ion meter (pH2100 Eutech).

Both conductivity and ISE measurements were performed in a thermostatted sample holder made of a double jacketed beaker connected to a water bath; the sample temperature was maintained at 25 ± 0.2 °C and was monitored by a Pt-100 resistor dipped in the sample and connected to a home-built resistance to temperature converter; SDS concentration was changed by adding known volumes of a suitable stock solution. Conductivity vs surfactant concentration plots were analyzed according to eq 1 as described in section 3.1.

ISE data were analyzed as described in ref 7; briefly, the degree of micelle ionization, α, was determined by fitting the Na^+ activity (α_{Na+}) collected above cmc to the equation $\alpha_{Na+} = (1 - \alpha)\mathrm{cmc} + \alpha c$ (where the cmc value was previously obtained by conductometry); below cmc α_{Na+} measured by the ISE is identical to the total surfactant concentration c.

2.2. Pulsed Field Gradient Spin−Echo (PGSE) NMR. Self-diffusion coefficient measurements have been carried out by the Fourier transform NMR pulsed field gradient spin−echo (PGSE−NMR) method.[8] Experiments were performed on a BS-587A NMR spectrometer (Tesla), operating at 80 MHz for protons, equipped with a pulsed field gradient unit (Autodif 504, STELAR s.n.c). The pulse sequence employed was the Stejskal-Tanner[9] sequence, 90°-τ-180°-τ-echo, with two rectangular field gradient pulses of about 0.25 T m^{-1} and duration δ, separated by a constant interval Δ. The echo amplitude recorded at 2τ is given by

$$A(2\tau) = \exp[-2\Delta/T_2]\exp[-\gamma^2 G^2 \delta^2(\Delta - \delta/3)D]$$

where T_2 is the spin−spin relaxation time, γ is the proton gyromagnetic ratio, and D is the self-diffusion coefficient of the species responsible of the spin−echo decay. The strength of the applied field gradient (G) was determined before each experiment by a separate calibration with pure DMSO. The value of the DMSO self-diffusion coefficient was from the literature.[10] The magnetic field was locked by an external D_2O lock signal for all the samples. The temperature of the samples was maintained at 298.0 ± 0.2 K by means of a built-in variable temperature control unit. The accuracy of the self-diffusion coefficients was within 4%.

2.3. Small-Angle X-ray-Scattering (SAXS). SAXS measurements were carried out with a HECUS SWAX-camera (Kratky) equipped with a position-sensitive detector (OED 50M) containing 1024 channels of width 54 μm. Cu Kα radiation of wavelength 1.542 Å was provided by a Seifert ID-3003 X-ray generator (sealed-tube type), operating at a maximum power of 2 kW. A 10-μm thick nickel filter was used to remove the CuKβ radiation. The sample-to-detector distance was 281 mm. The scattering path between the sample and the detector was kept under vacuum (P < 1 mBar) during the measurements to minimize scattering from the air. The Kratky camera was calibrated using silver behenate, which is known to have a well-defined lamellar structure (d = 58.48 Å).[11] Scattering curves were monitored in a **Q**-range from 0.01 to 0.55 $Å^{-1}$. The liquid samples were filled into 1 mm quartz capillary using a syringe. Measurements were done at 25 °C. The temperature was controlled by a Peltier element, with an accuracy of ±0.1 °C. All scattering curves (slit smeared data) were corrected for the empty cell contribution (quartz capillary) containing the correspondent H_2O/PC ratio. The data were slit desmeared by linear method.[12]

3. Results

3.1. Effect of PC on Micellization. Let us start this section with a lean review on the properties of PC/water mixtures. Propylene carbonate is a highly polar (dielectric constant = 65.1; dipole moment 4.94 Debye) aprotic solvent that at room temperature is only partially miscible with water (around 20%). Indeed, the phase diagram of the binary system PC/water has a wide miscibility gap extending from 20 to 92 PC wt %.[13] Many physicochemical properties of the PC/water mixture have been investigated by Courtot-Coupez and L'Her in the water rich[14] and water lean region.[15] Of particular interest for the present work is the viscosity η that was previously investigated by us in the water-rich region. Since η increases linearly with PC loading, in the following we will estimate it for all the relevant PC/water compositions according to the first-order polynomial of ref 6.

The influence of propylene carbonate on the critical micelle concentration (cmc) was investigated through conductivity (κ) measurements. Below cmc only dissociated surfactant monomers are present, while above the cmc the solution contains monomers and micelles with different molar conductivities (hereafter denoted as Λ_S and Λ_{mic}, respectively).[16,17] If the explored concentration range is short enough, then Λ_S, Λ_{mic}, and the monomer concentration above the cmc are fixed. Accordingly, the cmc can be determined in a κ vs c plot as the abscissa where the $d\kappa/dc$ changes from Λ_S to Λ_{mic}. However, micellization is not a sharp phase transition and the self-assembly sets in over a finite concentration range. This results in a gradual change in the slope of conductivity curve. Furthermore, in the case of micelles characterized by small aggregation number Λ_S and Λ_{mic} are not so different from each other. Due to the above-mentioned points, often the conductivity curve exhibits a weak curvature making the determination of cmc by visual inspection (or as intersection of two straight lines) difficult. Actually, such a situation was observed for SDS in PC/water mixture (see, for example, Figure SI-1 of the Supporting Information and Figure 1 of reference 6) and we have estimated the cmc by fitting the whole data set to the function proposed by Carpena:[18]

$$\kappa(c) = \Lambda_s c + \sigma(\Lambda_{mic} - \Lambda_s)\ln\left[\frac{1 + e^{(c - \mathrm{cmc})/\sigma}}{1 + e^{-\mathrm{cmc}/\sigma}}\right] \qquad (1)$$

where σ is a measure of the width of micellization. Although eq 1 has been derived on the basis of a physical model,[18] we

used it as a mere phenomenological model encapsulating the features of conductivity changes taking place upon micellization and avoiding the arbitrary definition of pre- and post-cmc regimes. Figure 1A shows the dependence of cmc on the composition of aqueous mixture (expressed as PC wt %). The cmc depends in a nonmonotonic way on the PC loading. Addition of propylene carbonate first slightly decreases the onset of micelle formation then, for PC > 10 wt %, induces an increase in the cmc. The dependence of Λ_S and Λ_{mic} on the aqueous mixture composition is shown in Figure 1B. The addition of PC results in a moderate decrease in the monomer molar conductivity. Actually, the viscosity η of the aqueous mixture increases upon PC loading[6] and the Walden's rule ($\Lambda_S\eta$ = constant)[19] roughly accounts for the decrease in Λ_S (Figure 1B). At variance, passing from pure water to concentrated PC/water mixture (PC = 19 wt %) doubles the Λ_{mic} value (Figure 1B).

The parameters governing the micelle molar conductivity can be easily understood in the limit of negligible interionic interactions (i.e., at infinite dilution). The net charge, Z, of a micelle depends on the aggregation number (N_{agg}) and on the degree of ionization α ($Z = N_{agg}\alpha$). At infinite dilution:[16]

$$\Lambda_{mic}^{\ 0} = \alpha\left(\frac{eFZ}{KT} D_{mic}^{\ 0} + \lambda_{Na+}^{\ 0}\right) = \frac{eFN_{agg}\alpha^2}{KT} D_{mic}^{\ 0} + \alpha\lambda_{Na+}^{\ 0} \quad (2)$$

where λ°_{Na+} is the limiting equivalent conductivity of sodium ion, and D°_{mic} is the micellar diffusion coefficient at infinite dilution; as usual e and F denote the elementary charge and the Faraday constant, respectively. The α-values determined by means of Na^+ selective glass electrode indicate that micelle ionization increases upon PC loading (Figure 1A). The other parameters entering eq 2 (N_{agg} and D°_{mic}) are somehow related to the size of the aggregates, a point that will be discussed in detail in the following sections.

3.2. Effect of PC on Micellar Size. Real-life formulations usually employ surfactants at high concentration (≫cmc). The formulation of the oil-in-water microemulsion successfully used to remove vinyl polymers from frescoes[5] is based on 5.32 wt % SDS in water.

Figure 2A shows the evolution of SDS and PC self-diffusion coefficients, measured through PGSE−NMR technique, upon PC dilution of this solution of SDS in water (SDS/water = 5.32/94.68 by weight). The PC loading results in an evident increase in the SDS diffusion and in a (less marked) reduction of the self-diffusion coefficient of propylene carbonate, which is always below the value found in PC/water binary mixtures (1×10^{-9} m^2s^{-1}; dashed line). In all the measurements the PGSE decays are strictly monoexponential indicating that molecular exchange between micelles and bulk is *fast* compared to the experimental time-scale (about 0.1 s).[20] Under this condition, the self-diffusion coefficient probed by PGSE−NMR experiment is an *apparent* diffusion coefficient given by[21]

$$D_{app} = P_{free}D_{free} + (1 - P_{free})D_{mic} \quad (3)$$

where P_{free} is the fraction of molecules moving in the continuous aqueous bulk with diffusion coefficient D_{free}, and D_{mic} is the self-diffusion coefficient of the micelle. According to eq 3, the increase in the SDS self-diffusion coefficient (D_{SDS}) could be explained either by an increase in the surfactant monomers in the continuous phase or by a decrease in the micellar hydrodynamic size. Upon PC loading, the concentration of SDS monomers passes through a minimum (see the dependence of the cmc on PC content, Figure 1A). Only above this minimum do we expect an increase in the fraction of surfactant free in the continuous phase (P_{free} in eq 3). On the other hand, the molar conductivity of monomer decreases continuously as the system is enriched in PC (Figure 2A); this suggests a decrease of D_{free} as well. Instead, the measured self-diffusion coefficient of SDS increases monotonically with PC loading (Figure 2). As a whole this evidence indicates that the monomer scarcely contributes to the observed surfactant diffusion. Selected samples were doped with tetramethylsilane (TMS), a compound that is barely soluble in water. The TMS self-diffusion coefficients were found to be almost equal to the D_{SDS} (data not shown). We interpret this fact as a strong indication that the measured D_{SDS} reflects the diffusion of the micelles. This in turn implies a noticeable increase in the micelles diffusion coefficient likely due to a conspicuous decrease in their size. To test such an interpretation, small-angle X-ray scattering (SAXS) represents an appropriate technique. SAXS probes the aggregate size on a length scale of few Å and is insensitive to the presence of surfactant monomers in the continuous phase. Figure 3 shows the intensity of scattered X-ray, $I(\mathbf{Q})$, normalized for the micellar volume fraction as a function of the scattering vector ($\mathbf{Q}$) for samples

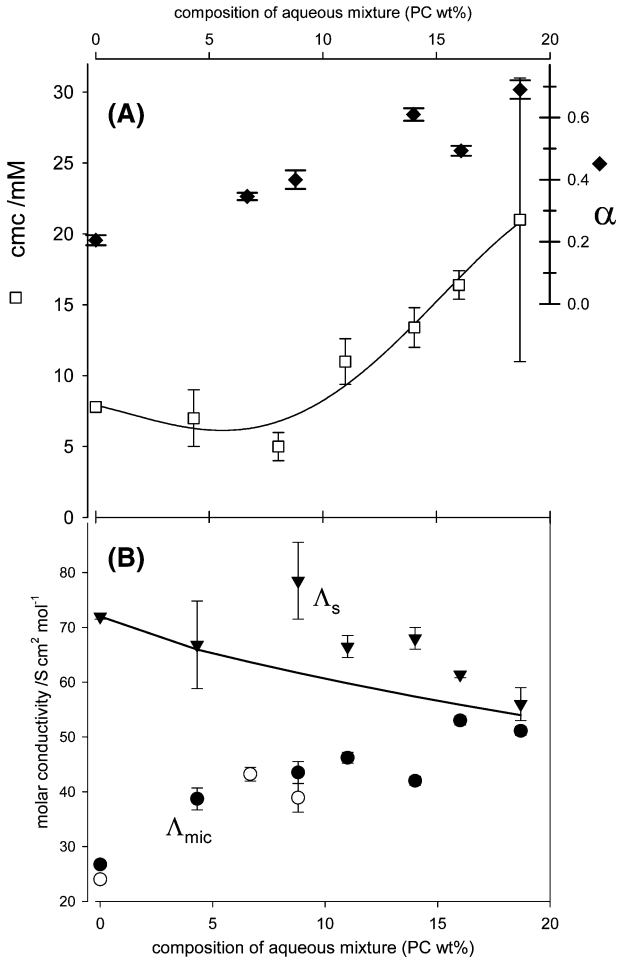

Figure 1. Conductometric parameters estimated by fitting conductivity data to eq 1 and ionization degree in PC/water mixtures. The abscissa is the weight composition % of aqueous mixture: $100 \times g_{PC}/(g_{PC} + g_{water})$. (A) left ordinate (□): values of critical micelle concentration; right ordinate (◆) micellar ionization degree (determined by means of ISE). (B) Molar conductivities of SDS monomer (▼) and micelle (●, ○) in PC/water mixtures. Continuous curve represents the prediction of Walden's rule for monomer conductivity (η values are from ref 6). Open symbols refer to Λ°_{mic} coming from the analysis of the dilution path described in section 3.3 (see also Supporting Information).

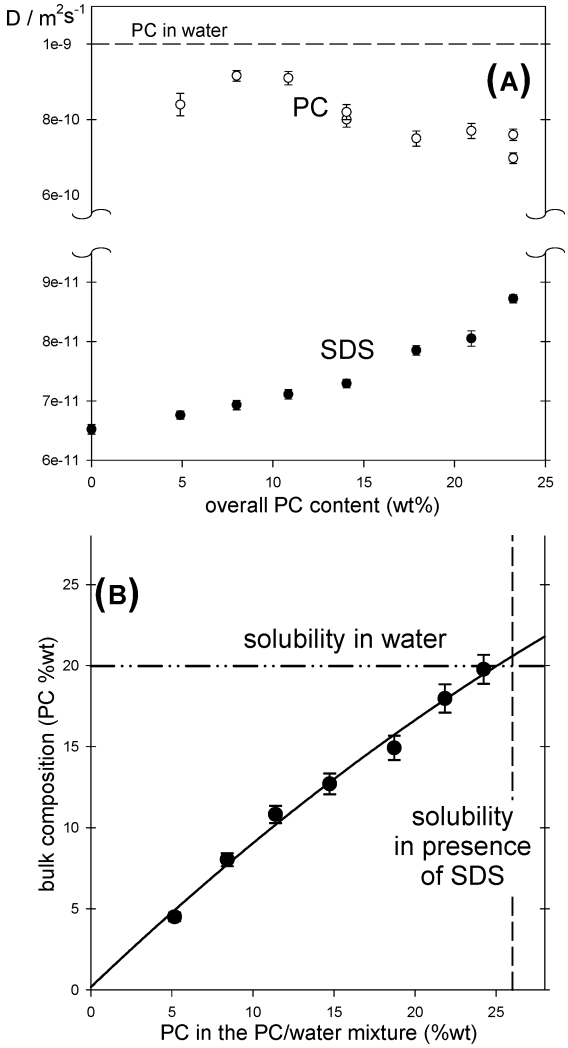

Figure 2. (A) Self-diffusion coefficients of SDS (●) and PC (○) along a PC dilution line (SDS/water= 5.32/94.68 by weight). Abscissa represents the overall weight content of PC in the system. Horizontal dashed line represents the diffusion constant of PC in binary PC/water mixtures (from ref 6). (B) Same samples as in panel A; comparison between the continuous bulk composition (ordinate) and the composition of aqueous phase expected if all the PC dissolves in water (abscissa). Bulk composition was estimated from the data of panel A using eq 3. The PC solubility in water (ordinate) and in SDS/water = 5.32/94.68 (abscissa) are also shown.

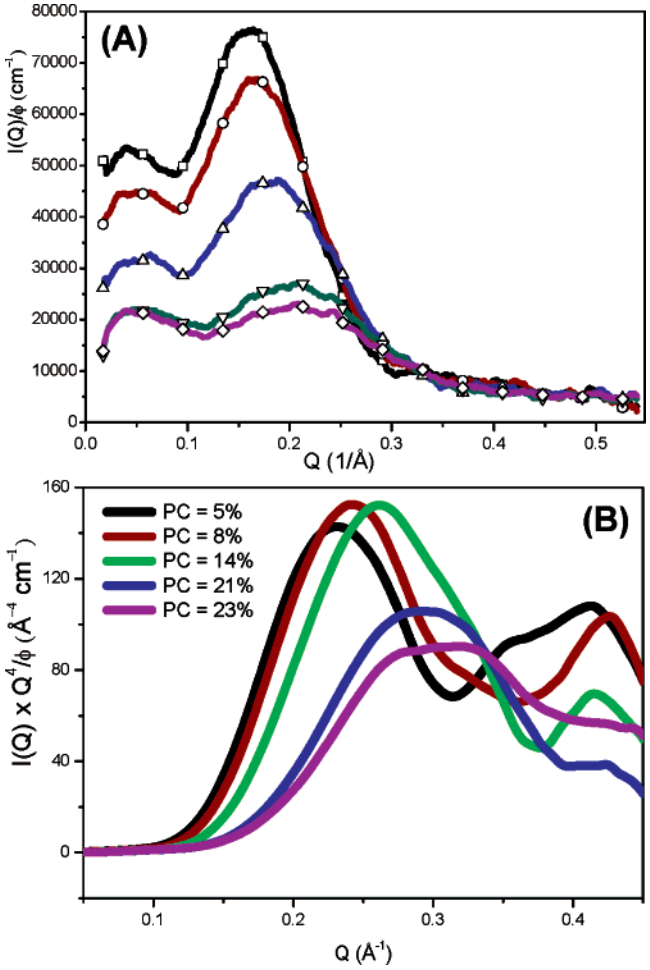

Figure 3. (A) SAXS curves ($I(\mathbf{Q})/\Phi$ vs $\mathbf{Q}$) for samples along a PC dilution line (SDS/water = 5.32/94.68 by weight; the overall weight content of PC in the system is indicated in the labels). (B) Kratky's plot ($\mathbf{Q}^4I(\mathbf{Q})/\Phi$ vs $\mathbf{Q}$) of the same data, vertical dashed lines indicates the position ($\mathbf{Q}^*$) of the first bump in this representation.

prepared by PC dilution of a 5.32 wt % SDS solution in water (the same dilution line investigated by means of PGSE−NMR in Figure 2). We defer the detailed analysis of the whole scattering curve to section 3.4; here, instead, we only focus on the main features that can be extracted from the SAXS spectra without the assumption of any precise model. All the curves in Figure 3A show an evident peak coming from the short-range local arrangement. The position of the peak maximum is expected to be inversely related to the average particle spacing.[22] As the amount of PC is increased, the position of the peak shifts toward larger values of the scattering vector **Q** (the average interparticle distance decreases) as shown in Figure 3A. This suggests that the effect of dilution with PC is an increase in the number of micelles consistent with the reduction of micellar size. When the scattering vector is much larger than the characteristic curvature of the interfaces, they appear flat at a length scale $\mathbf{Q}^{-1}$. Then the scattering intensity becomes proportional to the total area of the interfaces independently on the precise geometry of the phases. This is called the Porod's regime. However, when **Q** is as large as the curvature of interfacial film a deviation from the asymptotic Porod's law appears. General calculations indicate that $\mathbf{Q}^4I(\mathbf{Q})$ plotted as a function of **Q** exhibits at least one bump before reaching the Porod's plateau. This representation amplifies the oscillation due to the form factor reducing the contribution of the interparticle structure factor. The position of the bump is inversely related to the characteristic dimension of the colloidal aggregates independently of any precise structure model; hence, it is a very useful and general method of estimating it.[23] As clearly evidenced by Figure 3B for the investigated system, the position of such a bump moves toward larger **Q**-values as the amount of PC increases. The bump shift clearly indicates a consistent reduction of the aggregate dimensions upon PC loading.

As a matter of fact, and in agreement with PGSE−NMR measurements, the preliminary raw inspection of SAXS spectra, both in the standard and in the Porod representation, suggests that the main effect of PC is a reduction of the micellar size along with the increase of PC amount.

3.3. A Dilution Approach. According to the above results, the growth of SDS self-diffusion coefficient observed upon loading with PC should be attributed mainly to a decrease of the micelle's hydrodynamic size. Let us make a stronger assumption: the measured D_{SDS} fully reflects the micellar diffusion. The validity of such a hypothesis will be subsequently

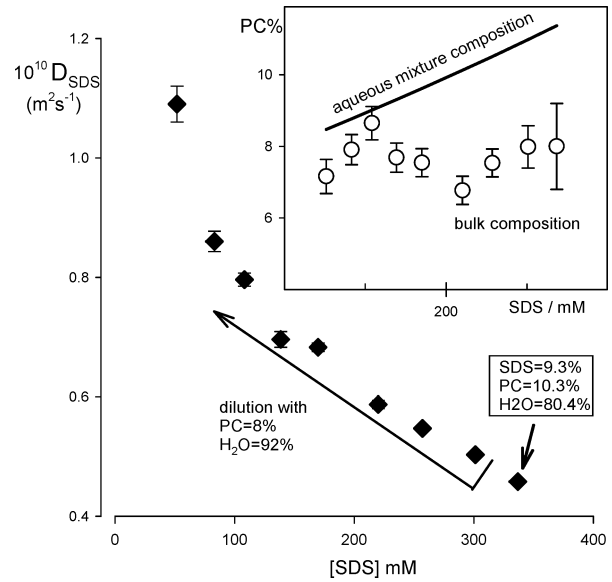

Figure 4. Dependence of SDS self-diffusion coefficients on the surfactant concentration along the suitable dilution path. A concentrated sample, prepared by dissolving SDS in a PC water solution (PC = 11. wt %) was diluted with an aqueous PC solution at PC = 8 wt %. Inset: composition of continuous bulk (% g_{PC} free/(g_{PC} free + g_{water})) as estimated by the analysis of D_{SDS} and D_{PC}; for comparison purposes the stoichiometric amount of PC in water (%g_{PC} total/(g_{PC} total + g_{water})) shown as solid line.

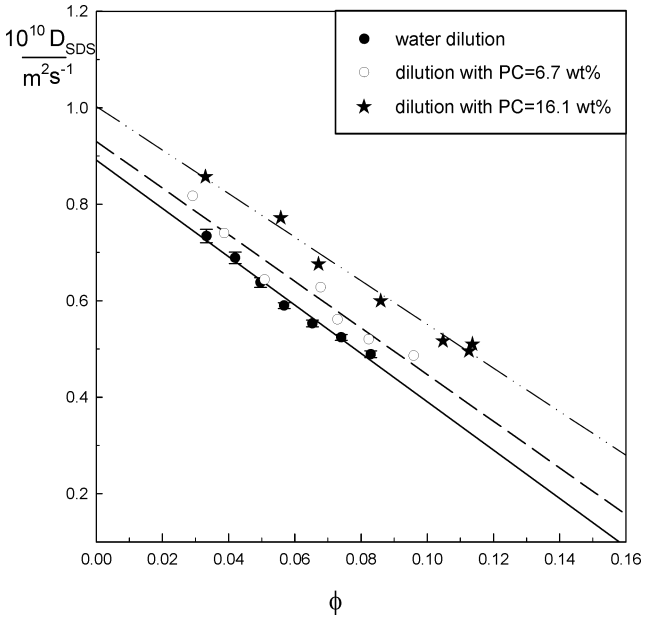

Figure 5. SDS self-diffusion coefficients measured along the relevant dilution paths (see text for details). Along each dilution path the system is composed by micelles with a constant ratio PC/SDS diluted by a continuous phase at constant composition (indicated in the legend). Straight lines are best fits according to eq 5; compositions of micellar and continuous phases and best fit parameters for five dilution paths are listed in Table 1, while for the sake of clarity, only three dilution lines are shown here.

checked for consistency with the results coming from independent SAXS experiments.

Propylene carbonate is soluble in water up to 20 wt % so the contribution of PC molecules dissolved in the aqueous bulk to the observed diffusion cannot be neglected. Under the postulation $D_{mic} = D_{SDS}$, the fraction of free PC molecules can be evaluated by applying eq 3 to the PC self-diffusion coefficient and setting D_{free} equal to the self-diffusion coefficient of PC in water ($\sim 10^{-9}$ m^2s^{-1} independent from the water content).[6] Once P_{free} is known, one can easily evaluate the composition of the aqueous phase because the amount of PC in the continuous phase is simply the product (total PC) × P_{free}. In Figure 2B, the actual composition of the aqueous continuous phase is reported as a function of the PC loading in the PC−water mixture. It is clear that the real PC concentration in the aqueous phase is always lower than the concentration inferred from the overall PC and water content. Of course, this reflects the presence of a relevant fraction of PC bound to the micelles. The data trend in Figure 2B suggests that the maximum solubility of PC in the micellar system (~27 PC wt % when expressed in terms of the overall PC and water content) is related to the PC−water solubility gap (20 PC wt %). Phase separation occurs upon dilution with PC when the continuous phase is saturated by propylene carbonate. This is different from the usual oil emulsification failure found in oil-in-water microemulsion when the micellar size satisfies the preferred interfacial curvature.[24] Since the viscosity of PC−water solutions increases upon PC loading, the growth of D_{SDS} data of Figure 2A should correspond to a dramatic drop in the micellar size. However, the knowledge of the viscosity of the continuous phase is not sufficient to estimate the aggregate's (hydrodynamic) size. Self-diffusion coefficients measured in PGSE−NMR experiments depend on direct and hydrodynamic interparticles interaction. It is only at infinite dilution, when interactions are missing, that the Stokes−Einstein equation holds:

$$D^{o}_{mic} = \frac{K_B T}{6\pi\eta R_h} \tag{4}$$

at finite concentration the measured self-diffusion coefficient is concentration dependent, and we can write (first-order approximation in volume fraction):[25]

$$D_{mic} = D^{o}_{mic}(1 + \lambda\phi) \tag{5}$$

The interaction constant λ takes into account changes in direct and hydrodynamics interparticle interactions upon dilution.

Unless λ is known a-priori (or evaluated by comparing self-diffusion and collective diffusion parameters),[6,26] the only way one has to retrieve the single particle diffusion coefficient (D°_{mic}), and thus the micellar size, is through a dilution procedure (according to eq 5). Clearly the presence of a cosolvent able to tune aggregate's size complicates the dilution approach. Actually unless the dilution path is duly chosen, self-assembled aggregates will continuously change their structure. However, the knowledge of the continuous-phase composition allows the selection of a suitable dilution path. Adding a solution with the same composition of the continuous phase (known from PGSE−NMR measurements) to the sample should leave the PC partition unchanged between the bulk and micelles and also the aggregate structure. According to the above consideration, we have undertaken a series of dilution experiments. A representative example is shown in Figure 4; here we start from a sample made of SDS (337 mM) dissolved in an aqueous mixture of PC (11.4 wt %) so that the overall composition by weight is SDS = 9.3%, PC = 10.3%, H_2O = 80.4%. According to the measured D_{SDS} and D_{PC}, the continuous phase is an aqueous solution with weight composition PC = 8 ± 1% and H_2O = 92 ± 1%. Therefore, the samples have been diluted with an aqueous solution with PC = 8.0%. The main panel of Figure 4 reports the D_{SDS} values measured along this dilution path. In the inset are reported the corresponding compositions of the continuous phase. It is clear that, within the experimental

TABLE 1: Self-Diffusion Coefficient at Infinite Dilution, Interaction Constant and Hydrodynamic Radii Inferred from Different Dilution Lines

bulk composition PC wt %	$(n_{PC}/n_{SDS})_{mic}$	$10^{11}D°_{mic}/m^2s^{-1}$	λ	η/mPa s[a]	R_h/Å[b]
0	0	8.9 ± 0.2	−5.6 ± 0.2	0.89	27.0 ± 0.5
6.8 ± 0.1	0.31 ± 0.05	9.3 ± 0.3	−5.2 ± 0.3	1.01	23.0 ± 0.8
7.9 ± 0.2	1.3 ± 0.1	9.9 ± 0.2	−4.8 ± 0.2	1.03	21.0 ± 0.5
13.3 ± 0.2	1.52 ± 0.06	9.9 ± 0.2	−4.5 ± 0.2	1.12	20.0 ± 0.5
16.2 ± 0.1	2.1 ± 0.1	10.0 ± 0.2	−4.5 ± 0.2	1.15	19.0 ± 0.4

[a] From ref 6. [b] From eq 4.

TABLE 2: Micellar Parameters Directly Obtained from the Fitting of SAXS Data (See Figure 6) Collected along a PC Dilution Line (SDS/water = 5.32/94.68 by Weight) at 298 K[a]

parameters	PC = 5%	PC = 8%	PC= 14%	PC = 21%	PC = 21%
			Fixed Parameters		
temperature (K)	298	298	298	298	298
ρ_{CORE} (Å^{-2})	7.74×10^{-6}	7.74×10^{-6}	7.74×10^{-6}	7.74×10^{-6}	7.74×10^{-6}
n_{PC}/n_{H20}[b,c]	9.105×10^{-3}	0.0147	0.0259	0.0385	0.0426
$(n_{PC}/n_{SDS})_{mic}$[c]	0.136612	0.411523	1.30378	3.07692	3.90625
ϵ[d]	78.7	78.5	78.1	77.8	77.7
ϕ	0.0442	0.0471	0.0553	0.0725	0.0795
ρ_S (A^{-2})	9.41×10^{-6}	9.4×10^{-6}	9.48×10^{-6}	9.53×10^{-6}	9.55×10^{-6}
			Fitted Parameters		
a (Å)	22 ± 1	22 ± 1	21 ± 1	19 ± 1	20 ± 1
b (Å)	15 ± 1	14 ± 1	13 ± 1	10 ± 1	9.5 ± 1
d (Å)	7.5 ± 0.8	7.2 ± 0.7	7.3 ± 0.7	9 ± 1	9 ± 1
I_{bkg} (cm^{-1})	428	571	605	583	576
Z	33 ± 2	30 ± 2	25 ± 2	13 ± 1	14 ± 1
			Derived Parameters		
ρ_{SHELL} (A^{-2})[e]	1.08×10^{-5}	1.08×10^{-5}	1.08×10^{-5}	1.03×10^{-5}	1.04×10^{-5}
N_{AGG}	62 ± 3	55 ± 3	46 ± 3	24 ± 2	23 ± 2
$\alpha = Z/N_{AGG}$	0.53 ± 0.05	0.54 ± 0.05	0.53 ± 0.05	0.54 ± 0.05	0.59 ± 0.06
$H = N_{H2O}/N_{SDS}$[f]	18 ± 2	17 ± 2	16 ± 2	29 ± 3	26 ± 3
R_H(Å)[g]	24.4 ± 1.5	23.5 ± 1.5	22.7 ± 1.5	21.4 ± 1.5	21.2 ± 1.5

[a] Samples are labeled by the overall PC content (wt %). The meaning of the parameters is described in section 3.4. [b] Continuous phase composition as mole ratio PC/water. [c] From PGSE−NMR measurements. [d] From ref 14. [e] The shell scattering length density was interactively calculated according to the fitted shell composition. [f] Deduced from the shell volume and $(n_{PC}/n_{SDS})_{mic}$ and α. [g] From eq 13.

error, the bulk composition is constant, and more important, it is different from the weight fraction based on the overall amount of PC and water. This is a first indication that the dilution path was properly chosen. It is only at infinite dilution (close to the cmc) that the stoichiometric composition of aqueous mixture equals the composition of the continuous phase. Accordingly, conductivity readings measured along the dilution path merge on the values taken in the cmc determination, i.e., loading with SDS a solution PC/water with fixed composition (see Figure SI-2 in the Supporting Information). Extrapolation to infinite dilution of dκ/dc furnishes the molar conductivity at infinite dilution of the micelles $\Lambda°_{mic}$.[27] The $\Lambda°_{mic}$ values measured for selected compositions of the aqueous phase (shown in Figure 1B as open dots) are very close to the Λ_{mic} found by fitting the data around the cmc to eq 1 (see the Supporting Information). In other words, we can approximate the Λ_{mic} values of Figure 1B to $\Lambda°_{mic}$. (we will take advantage of this point in the Discussion section).

The compositions of the continuous aqueous phase and of the micelles (strictly the mole ratio PC/SDS in the micelles, hereafter $(n_{PC}/n_{SDS})_{mic}$) for the five dilution lines investigated are listed in Table 1.

The micellar volume fraction ϕ was evaluated taking into account the micellized surfactant (c-cmc) and the fraction of PC within the micelle (1-P_{free}). The plots D_{SDS} versus ϕ follow reasonably a linear trend (at least for c > 10 cmc) as shown in Figure 5 and have been fitted to eq 5.

There are two main concerns about the analysis of self-diffusion coefficients collected along a dilution line, as those here proposed. The first is is the validity of eq 5. Such an equation foretells a linear dependence of D_{mic} on ϕ under two constraints: $D°_{mic}$ is constant (i.e., the dilution path is suitable) and λ is constant. λ depends on hydrodynamic and direct intermicelle interactions and should be sensitive to the changes in ionic strength implicit in the dilution procedures. The second point is related to the evaluation of micellar volume fraction. Strictly, ϕ in eq 5 should also take into account the bound water moving with the micelles.

With respect to these points, the fact that the plots D_{SDS} versus ϕ are linear is encouraging but not conclusive. The validity of the proposed approach will be confirmed in the Discussion section by comparison with the results from SAXS analysis.

The values of $D°_{mic}$ and λ obtained according to this approach are listed in Table 1 together with the viscosity of the dilution solution. From the single-particle self-diffusion coefficient a hydrodynamic size can be easily evaluated by means of the Stokes−Einstein relationship (eq 4). The micellar hydrodynamic radius decreases from 27 to 19 Å when the continuous phase passes from pure water to PC aqueous solution (PC = 16.1 wt %). This decrease in size is coupled to an increase in the $(n_{PC}/n_{SDS})_{mic}$ ratio. In other word, uptake of PC does not swell the micelle but instead shrinks it. Such a behavior is incompatible with the solubilization of PC within the apolar micellar core but can be accounted for by assuming that PC stays at the interface and increases in the mean SDS headgroup area. The size reduction is associated to a decrease of the repulsive interactions ($\lambda = -5.6$ in water; $\lambda = -4.5$ for PC = 16.1%).

We conclude this section with few words on the experimental limits of the dilution procedure. Since both D_{SDS} and D_{PC} are required, the echo decays of NMR resonances characteristic of

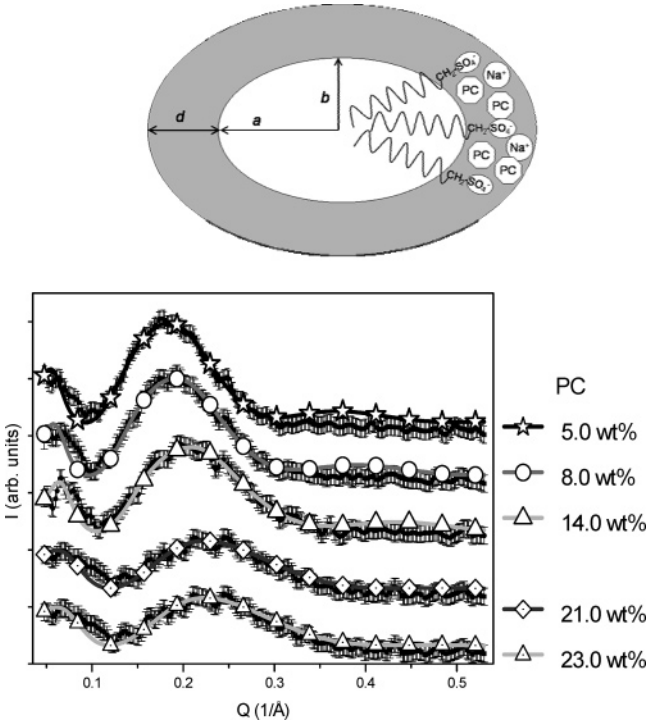

Figure 6. Upper panel: schematic model for the micellar structure (see section 3.4). Lower panel: desmeared SAXS spectra (markers) and correspondent fitting curves (full lines) for SDS/PC/water system as a function of PC wt % (SDS/water = 5.32/94.68 by weight; the overall weight content of PC in the system is indicated in the labels; same samples of Figure 3). For the sake of clarity, 21, 14, 8, and 5 PC wt % data and fittings are offset respectively by a 2000, 4000, 6000, and 8000 units on the intensity axis.

SDS and PC must be collected. This is relatively trivial when both the chemicals are present in comparable amounts or when the most concentrated component has a high self-diffusion coefficient, so that a proper choice of instrumental parameters (δ, Δ, and G; see section 2) results in echoes of comparable intensity. When the PC is in large excess its peaks tend to overlap the resonances of SDS, furthermore a high PC loading increases the micelles diffusion and D_{SDS} and D_{PC} become mutually close. Upon dilution (i.e., upon addition of aqueous solution of PC) the NMR signals of PC finally obscure the SDS resonances, so that D_{SDS} cannot be determined. With our experimental setup, this happened at PC ~17%. For higher PC loading, the system cannot be studied by the dilution procedure, instead a different approach, based on the comparison of PGSE−NMR and SAXS data collected at fixed high SDS concentration, can furnish considerable insight as will be described in the following section.

3.4. High PC Loading: Interpretation of SAXS Data. The analysis of PGSE−NMR data had allowed a considerable insight on the partition of PC between micelle and continuous phase. In particular, for the samples investigated by SAXS the self-diffusion coefficients of Figure 2 had permitted the evaluation of micelles and continuous phase composition (Table 2). This piece of information can be profitably used in the analysis of SAXS curves according to the following model.

The micellar solution is assumed to be composed of uniform-sized spheroidal micelles with a mean aggregation number, N_{agg}, and an effective charge *Z*. Micelles have been modeled as formed by a core−shell structure (see Figure 6). According to the results of previous section we assume that the bound PC is present only on the external hydrophilic shell of thickness *d*. This is formed by the polar heads, the first methylene group of SDS (according to ref 28), hydration water, a fraction of counterions, and the bound propylene carbonate molecules indicated by the PGSE−NMR measurements. The hydrophobic core of spheroidal shape, with principal axes *a*, *b*, ($a > b$), contains the surfactant hydrocarbon tails ($C_{11}H_{23}$), where the propylene carbonate cannot penetrate.

Within these assumptions the scattering intensity as a function of the wave vector **Q** can be written as[29]

$$I(\mathbf{Q}) = A(c - \mathrm{cmc})N(\sum_i b_i - V_m\rho_s)^2\tilde{P}(\mathbf{Q})\tilde{S}(\mathbf{Q}) + I_{bkg} \quad (6)$$

where *A* is the amplitude accounting for the instrumental factor (intensities are not in absolute scale), *c* is the surfactant concentration and cmc the critical micellar concentration (both in mol/L), b_i values are the X-ray scattering lengths of each atom of the surfactant and PC molecules, V_m is the volume per surfactant monomer considering also the PC coordinated molecules $V_m = V_{SDS} + V_{PC}(n_{PC}/n_{SDS})_{mic}$, and ρ_s is the scattering length density of solvent. $\tilde{P}(\mathbf{Q})$ is the orientationally averaged intraparticle structure factor for ellipsoidal particles, $\tilde{S}(\mathbf{Q})$ is the orientationally averaged center−center interparticle structure factor, and the additive term I_{bkg} takes into account the incoherent and instrumental background. $\tilde{P}(\mathbf{Q})$ is given by

$$\tilde{P}(\mathbf{Q}) = \int_0^1 |F(Q,\mu)|^2 d\mu \quad (7a)$$

The orientational-dependent form factor, $F(\mathbf{Q},\mu)$, is given by

$$F(\mathbf{Q},\mu) = f\frac{3j_1(u)}{u} + (1-f)\frac{3j_1(v)}{v} \quad (7b)$$

$$u = \mathbf{Q}[\mu^2a^2 + (1-\mu^2)b^2]^{1/2} \quad (7c)$$

$$v = \mathbf{Q}[\mu^2(a+d)^2 + (1-\mu^2)(b+d)^2]^{1/2} \quad (7d)$$

where μ takes into account the direction of the symmetry axis of the spheroid and the **Q** vector, $j_1(x)$ is a first-order Bessel function, *b* and *a* are the short and long principal axis of the ellipsoid, respectively. In eq 7b *f* is a dimensionless number given by

$$f = V_t(\rho_{core} - \rho_{shell})/(\sum b_i - V_m\rho_s) \quad (8)$$

where ρ_s is the scattering length density of the continuous phase constituted by H_2O and the fraction of PC that is not adsorbed at the micelle interface; this is a known quantity because the composition of aqueous phase was already resolved by PGSE−NMR (Table 2). The scattering length density of the micelle hydrophobic core is given as well because it is assumed to be composed of close packed hydrocarbon tails of dodecylsulphate; $\rho_{core} = [n_C b_C + 2(n_C + 1)b_H]/V_t$ where V_t is the volume of the surfactant "tail" in Å^3 given by Tanford equation for a linear carbon tail constituted of a number *n* of CH_2 residues $V_t = (26.9n - 27.4)$,[30] in the present case, $n = 11$.

The scattering length density of the micellar outer layer ρ_{shell} depends on the shell composition as

$$\rho_{shell} = N/V_{shell}[(Hb_{water}) + (1-\alpha)b_{Na^+} + b_{head} + b_{PC}(n_{PC}/n_{SDS})_{mic}] \quad (9)$$

where V_{shell} is the volume of spheroidal shell (depending on the geometrical parameters *a*, *b*, and *d*), α is the ionization degree $\alpha = Z/N_{agg}$, and $b_{head} = (1-\alpha)b_{Na^+} + Hb_{H_2O} + b_{CH_2SO_4^-}$. *H* is the hydration number accounting for the number of water

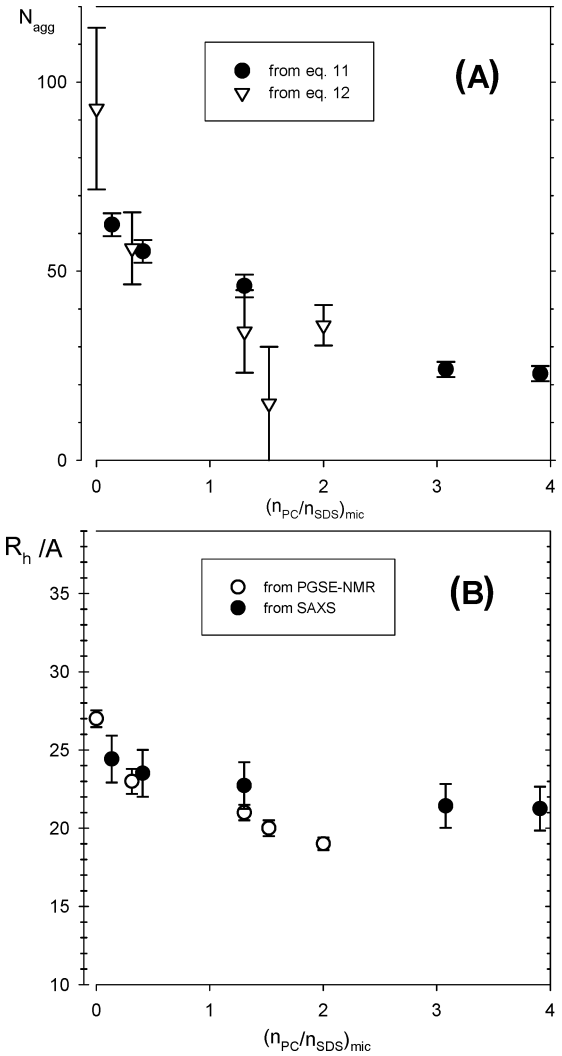

Figure 7. Aggregation number (panel A) and hydrodynamic radius (panel B) as a function of the micellar composition (see Discussion section). Open symbols were evaluated on the basis of PGSE−NMR data; closed symbols were evaluated on the basis of SAXS data.

molecules associated to the surfactant polar head defined as $H = [(V_{shell}/N) - (V_m - V_t) - \alpha V_{Na^+}]/V_{H_2O}$; finally, the mole ratio $(n_{PC}/n_{SDS})_{mic}$ was determined by PGSE−NMR (Table 2).

The orientationally averaged interparticle structure factor $\tilde{S}(\mathbf{Q})$ entering eq 6 is given by

$$\tilde{S}(\mathbf{Q}) = 1 + \frac{\langle |F(\mathbf{Q},\mu)| \rangle^2}{\langle |F(\mathbf{Q},\mu)|^2 \rangle} |S_{MM}(\mathbf{Q}) - 1| \qquad (10)$$

$S_{MM}(\mathbf{Q})$ has been calculated, as described by Liu et al.,[29] by solving the Ornstein−Zernicke equation for the pair correlation function within the nonadditive radius multicomponent mean spherical approximation closure that yields analytical solutions.

The experimental SAXS curves for five PC dilutions of a solution of SDS in water (SDS/water = 5.32/94.68 by weight) have been analyzed using a statistically weighted nonlinear least-square fitting according to the eqs 6−10 above. As input parameters (aside from temperature, ionic strength, and ρ_{core}) were used the compositions of aqueous and micellar phase and the related quantities: the micelle volume fraction (ϕ), the scattering length density of continuous phase (ρ_s) and the dielectric constant (ϵ) assumed to be equal to the dielectric constant of PC/water mixtures[14] of the same composition of continuous phase. For each sample the adjustable parameters

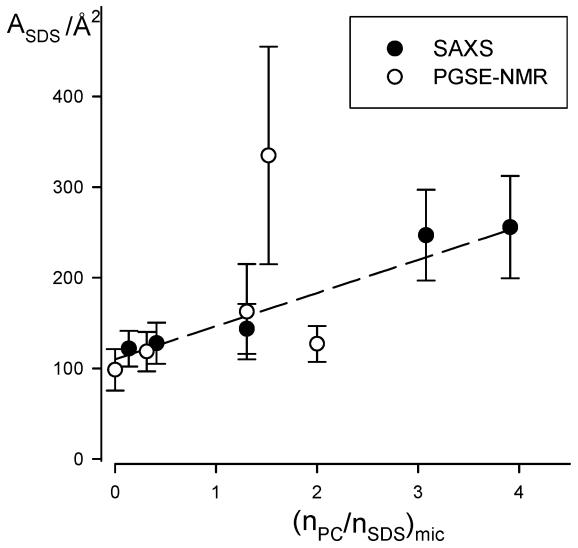

Figure 8. Mean polar head area of SDS evaluated through eq 14 using the data of Figure 7. Dashed line is the best fit according to eq 15.

were the major core radius a, the minor core radius b, the shell thickness d, the micellar charge Z (entering the structure factor) and the background contribution I_{bkg}; the amplitude A was assumed to be equal for all the samples so that the five scattering curves have been simultaneously fitted under this constraint. During the fitting procedure, the shell scattering length density was calculated iteratively exploiting the internal relations between micellar geometry, charge and the parameters of eq 9. The fits and the experimental data are compared in Figure 6, while the characteristic parameters are listed in Table 2.

4. Discussion

The geometrical parameters of the hydrophobic core of the micelles (Table 2) allow the evaluation of the mean number of SDS molecules within a micelle (the aggregation number N_{agg}). According to the model used to analyze SAXS curves, the spheroidal core has a volume equal to $4\pi a^2 b/3$ and is composed by close-packed tails so that

$$N_{agg} = \frac{4\pi a^2 b}{3V_t} \qquad (11)$$

Alternatively, the aggregation number can be evaluated without *any assumption on micelle shape and composition* through self-diffusion, conductivity and ISE data using eq 2 that can be arranged as

$$N_{agg} = \left(\frac{\Lambda_{mic}^{\ 0} - \alpha \lambda_{Na+}^{\ 0}}{eF\alpha^2 D_{mic}^{\ 0}} \right) KT \qquad (12)$$

The parameters $\Lambda^\circ_{mic} \approx \Lambda_{mic}$, α, and D°_{mic} have been determined separately in the independent experiments described in the Results sections 3.1 and 3.3. λ°_{Na+} was evaluated according to the observation that the molar conductivity of SDS monomer follows roughly the Walden's rule (Figure 1A). Therefore, we also assume that $\lambda^\circ_{Na+}\eta =$ constant and, knowing the limiting equivalent conductivity of sodium ion in water and the continuous phase viscosity, λ°_{Na+} was evaluated for each micelle composition. The aggregation number evaluated by means of the two independent approaches (viz. eqs 11 and 12) are compared in Figure 7A. It should be stressed that the two strategies are based on completely independent measurements

and assumptions. To compare N_{agg} values obtained from SAXS experiments at fixed composition with those obtained through extrapolation at infinite dilution along a dilution path, we have chosen as an independent variable $(n_{PC}/n_{SDS})_{mic}$. As shown in Figure 7A both approaches lead to N_{agg}-values mutually close and indicate that, within a micelle, a relevant decrease in the number of surfactant molecules parallels the uptake of propylene carbonate.

SAXS and PGSE−NMR results can be compared also in terms of hydrodynamic size as shown in Figure 7B. The hydrodynamic radii R_h are calculated directly from PGSE−NMR data of section 3.3 using the Stokes−Einstein relation (eq 4). The geometrical parameters obtained from SAXS experiments (viz. *a*, *b*, and *d*) can be rearranged to give the equivalent hydrodynamic radius expected for the prolate micelle modeled in section 3.4 according to[31]

$$R_h = \frac{a+d}{G(Y)};\ Y = \frac{b+d}{a+d}$$

$$G(Y) = [1 - Y^2]^{-1/2} \ln\left[\frac{1 + (1 - Y)^2}{Y}\right] \qquad (13)$$

Note that with both approaches the R_h is strictly an infinite dilution quantity. Also in the case of hydrodynamic size SAXS and PGSE−NMR give fully consistent results (Figure 7B). As a whole, Figure 7 indicates that binding of PC to the micellar surface induces a decrease in both the size and the aggregation number of the aggregate. This in turn implies a PC-induced expansion of the mean area occupied by a SDS molecule at the micelle interface A_{SDS} = (micelle surface)/N_{agg}. We can evaluate this quantity from the PGSE−NMR and SAXS results of Figure 7 as

$$A_{SDS} = \frac{4\pi R_{mic}{}^2}{N_{agg}} \qquad (14)$$

Two points of eq 14 should be stressed. First, the above equation defines an average polar head area (A_{SDS}) evaluated at the outer surface of the micelle, i.e., the hydrodynamic shear surface of micelles for PGSE−NMR measurements and the surface enveloping the solvated sulfate groups of the micellized detergent ions for SAXS data. Second, although, the above equation implicitly describes the micelles as a sphere with a radius equal to R_h, the numerical output also holds for the prolate spheroids of Table 2.[32] The dependence of the average polar head area on the amount of PC at the interface is shown in Figure 8, where a linear growth in the SDS polar head area upon $(n_{PC}/n_{SDS})_{mic}$ increase is evident. The simplest model describing such a behavior supposes additive contribution of PC and surfactant to the total slipping surface (micelle's area = $n_{SDS}\ a^\circ_{SDS} + n_{PC}\ a^\circ_{PC}$) so that the mean area per SDS headgroup is

$$A_{SDS} = \frac{\text{micelle's area}}{N_{agg}} = a^\circ_{SDS} + a^\circ_{PC}\left(\frac{n_{PC}}{n_{SDS}}\right)_{mic} \qquad (15)$$

where a°_{SDS} (a°_{PC}) is the contribution of a SDS (propylene carbonate) molecule to the micellar surface (evaluated at the slipping plane). The mean polar-group area calculated on the basis of the aggregation numbers coming from PGSE−NMR and SAXS data follows a straight line when plotted against the mole ratio PC/SDS within the micelle. Interestingly, the slope is 36 ± 3 Å^2 with values that agree well with the surface occupied by a sphere of volume equal to the PC molecular volume (33 Å$^2 = \pi(3v_{PC}/4\pi)^{2/3}$; v_{PC} = 142 Å^3). Such an increase in surfactant headgroup area accounts also for the increase in the degree of micelle ionization (α, Figure 1) and for the decrease in the repulsive interactions (λ, Table 1) found upon PC loading. Indeed, both the counterions binding and the repulsive interactions are enhanced by an high charge density of the micelle and are expected to drop upon increasing the mean area occupied by the charged surfactant headgroup.

5. Conclusions

The study of micellar systems in presence of a cosolvent able to partition themselves between the continuous phase and micelles presents considerable difficulties. Scattering and self-diffusion results contain information on both interparticles interactions and particle size and shape. In the present work we have presented a strategy based on PGSE−NMR measurements that allows, through the identification of the suitable dilution path, the evaluation of hydrodynamic size of the micelles at infinite dilution (where hydrodynamic and direct interactions are negligible). Furthermore, a method for the direct determination of the aggregation number of ionic micelles without any assumption on their shape and composition was presented. However, at very high PC/SDS ratio, the dilution approach cannot be used. Therefore, SAXS data collected at fixed composition have been fitted to a reasonable model (troublesome hydrodynamic interactions are not involved in the interpretation of SAXS data). The knowledge of PC partition (obtained by independent PGSE−NMR measurements) has allowed the reduction of best-fit parameters. Both the strategies consistently indicate that PC acts as a cosurfactant for the SDS micelles decreasing their size and aggregation number by increasing the mean headgroup area of the surfactant. As a consequence the effective micellar charge decreases and the intermicelle interactions are less repulsive. We retain that the strategies here presented could be applied to the study of other cosolvents (e.g., urea) to investigate their effect on self-assembled aggregates.

Acknowledgment. We are grateful to Prof. Maurice L'Her for sharing with us his knowledge on the properties of PC/water mixtures. This work was supported by the MIUR of Italy (PRIN 2003 prot. 2003035197**;** PRIN 2005 prot. 2005027011) and by the Consorzio Interuniversitario per lo sviluppo dei Sistemi a Grande Interfase (CSGI-Firenze).

Supporting Information Available: Additional details about the representative conductivity and ion-selective electrode (ISE) measurements. This material is available free of charge via the Internet at http://pubs.acs.org.

References and Notes

(1) Hiemenz, P. C.; Rajagopalan, R. *Principles of Colloid and Surface Chemistry*, 3rd ed; Marcel Dekker: New York, 1997; pp 331−338.

(2) Evans, D. F.; Wennerström, H. *The Colloidal Domain*; VCH: New York, 1994; Chapter 3.

(3) See, for example, Wetlaufer, D. B.; Malik, S. K.; Stoller, L.; Coffin, R. L. *J. Am. Chem. Soc.* **1964**, *86*, 508. Enea, O.; Jolicoeur, C. J. *J. Phys. Chem.* **1982**, *86*, 3370. Baglioni, P.; Ferroni, E.; Kevan, L. *J. Phys. Chem.* **1990**, *94*, 4296. Breslow, R.; Guo, T. *Proc. Natl. Acad. Sci. U.S.A.* **1990**, *87*, 167. Abuin, E. B.; Lissi, E. A.; Aspée, A.; Gonzales, F. D.; Varas, J. M. *J. Colloid Interface Sci.* **1997**, *186*, 332.

(4) Baglioni, P.; Rivara-Minten, E.; Dei, L.; Ferroni, E. *J. Phys. Chem.* **1990**, *94*, 8218.

(5) Carretti, E.; Dei, L.; Baglioni, P. *Langmuir* **2003,** *19*, 7867. Carretti, E.; Salvadori, B.; Baglioni, P.; Dei, L. *Stud. Conserv.* **2005**, *50*, 128.

(6) Palazzo, G.; Fiorentino, D.; Colafemmina, G.; Ceglie, A.; Carretti, E.; Dei, L.; Baglioni, P. *Langmuir* **2005**, *21*, 6717.

(7) Hsiao, C. C.; Wang, T. Y.; Tsao, H. K. *J. Chem. Phys.* **2005**, *122*, 144702.

(8) Stilbs, P. *Prog. NMR Spectrosc*. **1987**, *19*, 1.

(9) Tanner, J. E.; Stejskal, E. O. *J. Chem. Phys.* **1968**, *49*, 1768.

(10) Holz, M.; Mao, X.; Seiferling, D.; Sacco, A. *J. Chem. Phys*. **1996**, *104*, 669.

(11) Blanton, T.; Huang, T. C.; Toraya, H.; Hubbard, C. R.; Robie, S. B.; Louer, D.; Gobel, H. E.; Will, G.; Gilles, R.; Raftery, T. *Powder Diffr*. **1995**, *10*, 91.

(12) Singh, M. A.; Ghosh, S. S.; Shannon, R. F. *J. Appl. Cryst.* **1993**, *26*, 787.

(13) Catherall, N.; Williamson, A. *J. Chem. Eng. Data* **1971**, *16*, 335. Grassi, S.; Dei, L. *J. Phys. Chem.* **2006**, *110*, 12191.

(14) Courtot-Coupez, J.; L'Her, M. *C. R. Acad. Sci. Paris C* **1972**, *275*, 103.

(15) Courtot-Coupez, J.; L'Her, M. *C. R. Acad. Sci. Paris C* **1972**, *275*, 195.

(16) Evans, H. C. *J. Chem. Soc.* **1956**, 579.

(17) Shanks, P. C.; Franses, E. I. *J. Phys. Chem.* **1992**, *96*, 1794 and references therein.

(18) Carpena, P.; Aguiar, J.; Beranola-Galvàn, P.; Carnero Ruiz, C *Langmuir* **2002**, *18*, 6054.

(19) Walden, P. *Z. Phys. Chem.* **1906**, *55*, 207.

(20) In the case of slow exchange the observed echo decay is the superimposition of the decays due to molecules in the two sites (i.e., it is two-exponential).

(21) Nilsson, P. G.; Lindman, B. *J. Phys. Chem.* **1983**, *87*, 4756. Nilsson, P. G.; Lindman, B. *J. Phys. Chem*. **1984**, *88*, 5391.

(22) Chen, S.-H.; Sheu, E.-Y.; Klaus, J.; Hoffmann, H. *J. Appl. Cryst*. **1988**, *21*, 751.

(23) Auvray, L.; Auroy, P. in *Neutron, X-Ray and Light Scattering*; Lindner, P., Zemb, T., Ed.; Elsevier: Amsterdam, 1991.

(24) Safran, S. A. *Statistical Thermodynamics of Surfaces, Interfaces and Membrane*; Addison-Weseley Publishing Company: New York, 1994; Chapter 8. Olsson, U.; Wennerstöm, H. *Adv. Colloid Interface Sci*. **1994**, *49*, 113.

(25) Cichocki, B.; Felderhof, B. U. *Phys. Rev. A* **1990**, *42*, 6024. Cichocki, B.; U. Felderhof, B. U. *J. Chem. Phys.* **1991**, *94*, 556.

(26) Galantini, L.; Giampaolo, S. M.; Mannina, L.; Pavel, N. V.; Viel, S. *J. Phys. Chem. B* **2004**, *108*, 4799.

(27) At low (but still finite) concentration the equivalent conductivity of an electrolyte follows the Kohlrausch's law, i.e., $\Lambda = \Lambda^\circ - A\sqrt{c}$ (where the constant A is independent on the concentration c). In terms of specific conductivity one has $\kappa = \Lambda^\circ c - Ac^{3/2}$ and further differentiation with c leads to $(d\kappa/dc) = \Lambda^\circ - {}^3/_2 A\sqrt{c}$. Accordingly, $d\kappa/dc$, above the cmc, follows a straight line with intercept equals to the molar conductivity at infinite dilution of the micelles Λ°_{mic}.

(28) Zemb, T.; Charpin, P. *J. Physique* **1985**, *46*, 249.

(29) Liu, Y. C.; Baglioni, P.; Teixeira, J.; Chen, S.-H. *J. Phys. Chem*. **1994**, *98*, 10208.

(30) Tanford, C. *J. Phys. Chem.* **1972**, *76*, 3020.

(31) Perrin, F. *J. Phys. Radium* **1934**, *5*, 497.

(32) The prolate spheroid surface can be calculated from the minor and major axes. The corresponding surfactant head-group area $A_{SDS} = 2\pi/N_{agg}[(b + d)^2 + ((a + d)(b + d))/\sqrt{1-((b+d)^2)/(a+d)^2}\ \sin^{-1}(\sqrt{1-((b+d)^2)/(a+d)^2})]$ equals, for the parameters of Table 2, within 0.2% the A_{SDS} evaluated according equation 14.